Journal of Magnetic Resonance 333 (2021) 107101

Contents lists available at ScienceDirect

Journal of Magnetic Resonance

journal homepage: www.elsevier.com/locate/jmr

NMR of ^{31}P nuclear spin singlet states in organic diphosphates

Stephen J. DeVience [a,1,*], Ronald L. Walsworth [b,c,2], Matthew S. Rosen [c,d]

[a] Department of Chemistry and Chemical Biology, Harvard University, 12 Oxford St., Cambridge, MA 02138, USA
[b] Harvard-Smithsonian Center for Astrophysics, 60 Garden St., Cambridge, MA 02138, USA
[c] Department of Physics, Harvard University, 17 Oxford St., Cambridge, MA 02138, USA
[d] Athinoula A. Martinos Center for Biomedical Engineering, Massachusetts General Hospital, 149th Thirteenth St., Charlestown, MA 02129, USA

ARTICLE INFO

Article history:
Received 16 September 2021
Revised 27 October 2021
Accepted 28 October 2021
Available online 30 October 2021

Keywords:
Phosphorus NMR
Nuclear spin singlet state
Quantum filter

ABSTRACT

^{31}P NMR and MRI are commonly used to study organophosphates that are central to cellular energy metabolism. In some molecules of interest, such as adenosine diphosphate (ADP) and nicotinamide adenine dinucleotide (NAD), pairs of coupled ^{31}P nuclei in the diphosphate moiety should enable the creation of nuclear spin singlet states, which may be long-lived and can be selectively detected via quantum filters. Here, we show that ^{31}P singlet states can be created on ADP and NAD, but their lifetimes are shorter than T_1 and are strongly sensitive to pH. Nevertheless, the singlet states were used with a quantum filter to successfully isolate the ^{31}P NMR spectra of those molecules from the adenosine triphosphate (ATP) background signal.

© 2021 Elsevier Inc. All rights reserved.

1. Introduction

Organophosphates play a critical role in biology as energy carriers. Adenosine triphosphate (ATP) is the main currency of energy for the cell and is central to cellular metabolism [1,2]. Energy is released and used to drive metabolic processes by breaking the phosphate-phosphate bond, producing adenosine diphosphate (ADP) and inorganic phosphate. At the same time, new ATP is created from ADP via glycolysis, the citric acid cycle, and the electron transport chain, all driven by the breakdown of sugars, fatty acids, and proteins. ATP concentration *in vivo* is typically several times that of ADP, and their ratio provides information about cellular energy status and mitochondrial function [3,4]. Another organophosphate, nicotinamide adenine dinucleotide (NAD), is a cofactor for many metabolic pathways in which it is converted between its oxidized form NAD^+ and its reduced form NADH. The ratio between NAD^+ and NADH reflects the oxidoreductive state of the cell [5], and the total NAD concentration can change as a result of aging and neurodegenerative disease [6].

In vivo ^{31}P NMR spectroscopy and imaging are commonly used to quantify the relative concentrations of ATP, ADP, and NAD noninvasively. Applications include the assessment of traumatic brain injury, investigation of aging, and diagnosis of musculoskeletal diseases [7–11]. However, detection and quantitation of these molecules can be difficult due to spectral overlap, particularly in the −11 to −12 ppm spectral region where lines from ATP, ADP, and NAD all occur. While some lines can easily be resolved with high-field, high-resolution NMR spectroscopy [10,12], lower field strengths used for human MRI make this challenging; thus ADP concentration is often calculated indirectly based on measurements of phosphocreatine [13,14].

To help isolate such overlapping spectral lines, quantum filters and spectral editing pulse sequences can be used to eliminate background signals. While widely used in ^{1}H NMR spectroscopy, there are few examples for ^{31}P. Jayasunder *et al.* used a multiquantum filter to remove interfering 2,3-diphosphoglycerate signal from measurements of inorganic phosphate [15], and Tsai *et al.* used double-quantum filtered HETCOR to study dentin with solid-state NMR [16]. Brindle *et al.* used spectral editing to suppress phosphomono- and phosphodiester signals [17]. Berkowitz and Ben-Bashat *et al.* explored ^{31}P-^{1}H quantum coherences for the measurement of ADP in the presence of ATP *in vitro* [18,19]. A drawback is that ADP appears as an anti-phase signal, which

ADP, adenosine diphosphate; ATP, adenosine triphosphate; NAD, nicotinamide adenine dinucleotide; SAR, specific absorption rate; CSA, chemical shift anisotropy.

* Corresponding author.
E-mail addresses: stephen@scalarmag.com (S.J. DeVience), walsworth@umd.edu (R.L. Walsworth), msrosen@mgh.harvard.edu (M.S. Rosen).
[1] Present address: Scalar Magnetics, LLC, 3 Harolwood Ct., Apt C, Windsor Mill, MD 21244, USA.
[2] Present address: Quantum Technology Center, University of Maryland, 8228 Paint Branch Dr., College Park, MD 20742, USA.

https://doi.org/10.1016/j.jmr.2021.107101
1090-7807/© 2021 Elsevier Inc. All rights reserved.

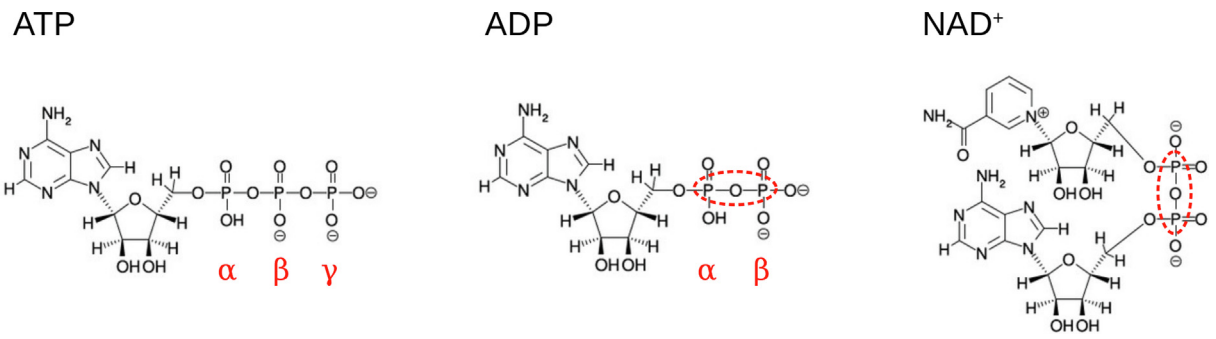


Fig. 1. Structures of ATP, ADP, and NAD^+. Singlet order can be prepared on the ^{31}P pairs of ADP and NAD^+ (circled). The triphosphate group of ATP does not support a singlet, because as a spin-0 state, the singlet must be composed of an even number of coupled spin-1/2 nuclei.

can lose intensity if T_2^* is short. More recently, Ren *et al.* used spectral editing to improve the NAD^+ spectrum near an interfering ATP peak. This involved subtracting an inversion spectrum from a reference spectrum, with the inversion time selected to null either the ATP or NAD^+ signal [20]. This decreased the ATP signal but did not fully remove it or other underlying lines such as uridine diphosphate glucose.

Recently, a new class of quantum filters and spectral editing techniques have been developed based on the long-lived nuclear spin singlet state [21–26]. The singlet state can be created in pairs of coupled nuclear spins when the spins are in the magnetically equivalent or near-equivalent conditions. This condition can be satisfied when the chemical shift is small relative to scalar coupling, such that $\Delta\nu \ll J$, or through the application of decoupling via CW spin-locking or a pulse train. The resulting singlet states can potentially have long lifetimes far beyond T_1 and can also be isolated from other signals via appropriate pulse sequences. The structure of ADP and NAD, each with a pair of phosphate groups on which ^{31}P-^{31}P singlet order can be prepared, appear to lend themselves to such a detection strategy (Fig. 1).

To test this method, we created singlet states in the ^{31}P pairs of ADP and NAD^+. We measured the longitudinal relaxation time (T_1) and singlet relaxation time (T_S) under both neutral and basic conditions. We then used a singlet quantum filter via the SUCCESS sequence [21] to isolate the ADP and NAD^+ spectra in the presence of a large ATP background.

2. Results

^{31}P NMR spectra and measurements of T_1 and T_S were acquired for ADP and NAD^+ (50 mM in pH 7.0 phosphate buffer) at 4.7 T (81 MHz ^{31}P frequency). The spectrum of ADP consisted of two pairs of widely split lines typical of the weak coupling condition, with $\Delta\nu = 128.9$ Hz and $J_{PP} = 21.2$ Hz. NAD^+ exhibited a second-order pattern reflecting a much smaller frequency difference, with $\Delta\nu = 24.2$ Hz and $J_{PP} = 20.2$ Hz. T_1 times were between 2.5 and 2.9 s, while T_S was ~ 500 ms for ADP and 1.35 s for NAD^+ (Table 1), giving ratios $T_S/T_1 \approx 0.2$ and $T_S/T_1 \approx 0.5$ for ADP and NAD^+, respectively. The singlet lifetime is clearly not long-lived and is in fact significantly shorter than T_1, possibly due to strong relaxation from nearby proton spins interacting asymmetrically with the phosphorus nuclei [27]. At pH 7, the β-ADP phosphate group (pK_a = 0.9 and 2.9–4.4) and the NAD^+ phosphate groups ($pK_a \sim 2$) are >99.7% unprotonated, but the α-ADP phosphate group (pK_a = 6.8–7.2) remains partially protonated, likely driving ^{31}P T_1 relaxation [28–30]. Given pH = 7 and pK_a = 6.8, 39% of α-ADP groups are protonated at a given time. To measure singlet lifetime with these protons fully removed, a basic 50 mM ADP solution was prepared in 0.5 M sodium hydroxide solution, giving a pH > 13 and dissociating over 99.99% of the protons from the α-ADP phosphate group. This increased T_1 significantly and T_S by a factor of eight (Table 1). However, T_S/T_1 was still on the order of unity, indicating that other relaxation processes are also significant, likely from anti-correlated chemical shift anisotropy [31].

Next, we tested the ^{31}P SUCCESS sequence on a mixture containing 30 mM ATP, 3 mM ADP, and 3 mM NAD^+ in a pH 7.0 phosphate buffer. Fig. 2a shows a spectrum of the mixture measured with a 90°-FID sequence. Both ATP and ADP exhibit splitting patterns indicating weakly coupled ^{31}P groups (additional ATP peaks at −20 ppm are not shown), and the ADP peaks are on the shoulders of the ATP peaks. One of the NAD^+ peaks lies directly beneath an ATP peak while the other is resolved. Fig. 2b shows the results after using the SUCCESS sequence to target ADP. Using line fitting for quantitation, we find that 35% of the ADP signal is retained, compared with only 1% of the ATP signal, resulting in a factor of 35-fold enhancement for ADP signal contrast. Fig. 2c shows the results after targeting NAD^+ instead. For NAD^+, 43% of the signal is retained, compared with only 1.7% of the ATP signal, resulting in a factor of 25-fold enhancement for NAD^+ signal contrast.

3. Discussion and conclusion

Our results show that it is possible to create, and detect with NMR, nuclear spin singlet states on pairs of ^{31}P nuclei in common biomolecules. However, these singlet states relax significantly faster than T_1 under typical conditions, similar to the results reported by Korenchan *et al.* in tetrabenzyl pyrophosphate [31]. Measurements under basic conditions show that nearby protons are partly to blame, but their removal does not necessarily lead to a long-lived state. The strongest relaxation mechanism is likely chemical-shift anisotropy (CSA), which is absent in ^1H systems but is often strong in ^{13}C, ^{15}N, and ^{31}P systems [27,31,32]. Long-lived singlets can still be created in ^{13}C and ^{15}N pairs when molecules are small and highly symmetric. While it is possible that ^{31}P systems with the appropriate criteria also exist, rotation about the single bonds connecting phosphate groups makes it unlikely for this class of molecules.

Despite the short singlet lifetime, the SUCCESS sequence performed well at removing ATP background NMR signal and isolating the spectra of ADP and NAD^+. This method is potentially useful for *in vivo* MR spectroscopy at lower 1.5 T and 3 T magnetic field strengths typical of human and animal imaging, particularly when the broader lines *in vivo* lead to stronger spectral overlap. As a special case of zero-quantum filters, singlet filtration techniques such as SUCCESS and others are not significantly affected by B_0 inhomogeneity. While we based our technique on the Sarkar three-pulse sequence for singlet preparation and readout [33], other sequences such as M2S, SLIC, and APSOC might be more appropriate at lower

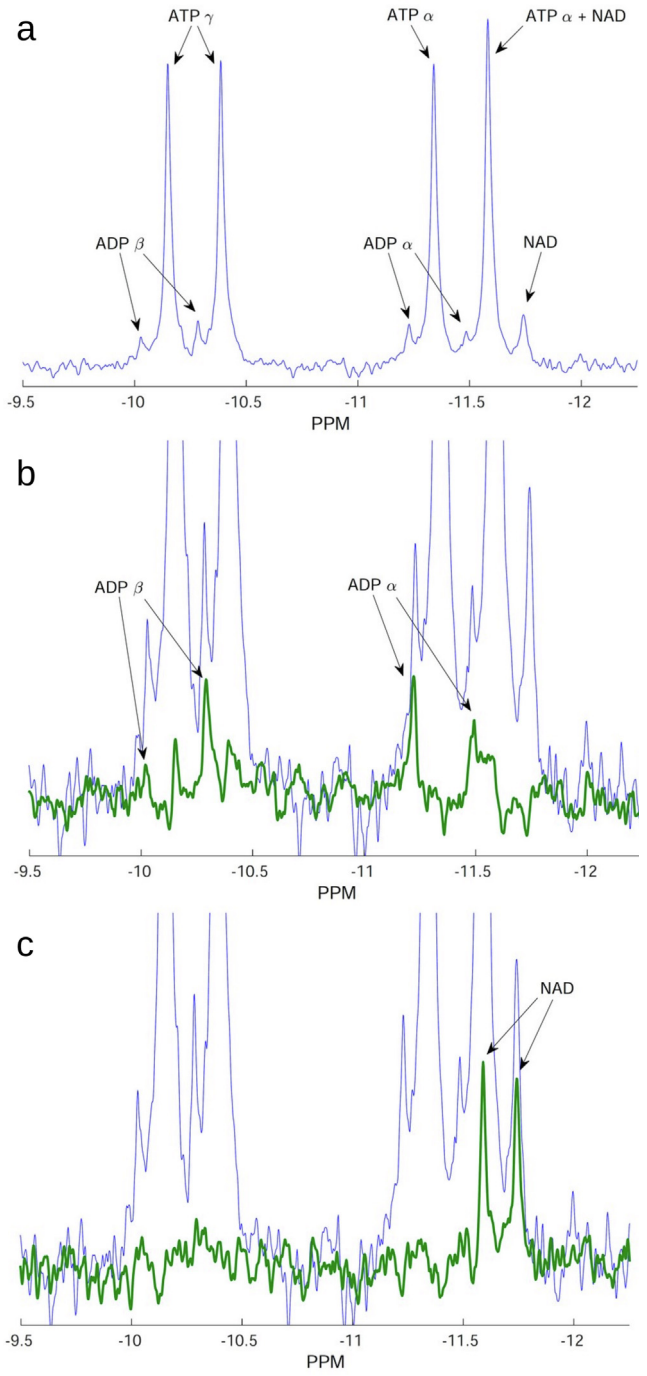


Fig. 2. (a) ^{31}P NMR spectrum of a mixture containing 30 mM ATP, 3 mM ADP, and 3 mM NAD$^+$ in a pH 7.0 phosphate buffer, measured with a 90-FID sequence (128 scans). ADP and NAD$^+$ signals are not fully resolved from ATP. (b) SUCCESS ^{31}P NMR spectrum of the same sample targeting ADP eliminates 99% of the ATP signal, allowing three of the four ADP peaks to be resolved (8192 scans). (c) SUCCESS ^{31}P NMR spectrum of the same sample targeting NAD$^+$ eliminates ATP and ADP signals, retaining only the NAD$^+$ doublet (8192 scans).

magnetic field strengths, especially for NAD$^+$, whose spins enter the nearly-equivalent regime at 1.5 T [34–36]. In that regime, it might be possible to also eliminate spin-locking for singlet preservation, so that specific absorption rate (SAR) can be minimized. The SUCCESS sequence can also be improved by using gradients as part of the quantum filter for isolating singlet state, but these were not available on our spectrometer. The use of phase cycling alone can

Table 1
Measured ^{31}P longitudinal and singlet lifetimes for ADP and NAD$^+$ (50 mM) at 4.7 T (81 MHz ^{31}P frequency).

Molecule	T_1 (s)	T_S (s)	T_S/T_1
ADP-α neutral	2.6 ± 0.2	0.49 ± 0.03	0.19 ± 0.02
ADP-β neutral	2.5 ± 0.1	0.53 ± 0.01	0.22 ± 0.01
ADP-α basic	3.9 ± 0.2	3.9 ± 0.7	1.0 ± 0.1
ADP-β basic	7.7 ± 0.3	4.2 ± 0.3	0.55 ± 0.04
NAD$^+$ neutral	2.9 ± 0.1	1.35 ± 0.01	0.47 ± 0.01

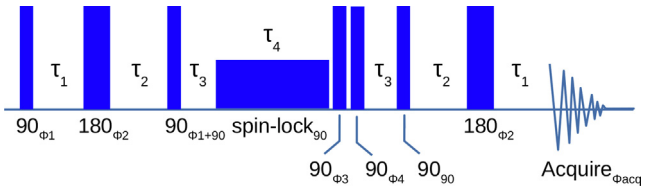


Fig. 3. SUCCESS sequence for singlet state creation, filtration, and readout. Delays τ_1, τ_2, and τ_3 are optimized to produce maximal singlet order on the target molecule and minimal singlet order in background molecules. Spin-locking is applied with a nutation frequency $\nu_n \geq 5\Delta\nu$, and spin-locking time τ_4 can be varied to measure singlet lifetime or to create further contrast.

lead to imperfect signal cancellation if there are small frequency shifts during acquisition, which might be why some ATP signal remained in both cases.

Besides SAR, another drawback for human imaging is the two to three-fold signal loss that results from relaxation and from quantum mechanical limitations of using a singlet filter. To attain the same signal-to-noise ratio as a conventional scan would require either four to nine times more averages or the use of voxels with two to three times the volume. However, current spectral editing techniques for NAD$^+$ also have a time penalty, as they require two scans, one reference and one with an inversion. While relaxation times are shorter *in vivo*, for NAD$^+$ we do not expect longitudinal or singlet relaxation to be significantly worse. Given that T_1 of up to 2 s has been measured in the brain at 7 T, $T_S \sim 1$ s is expected, which is still sufficiently long compared to the sequence time. The ^{31}P T_2 of NAD$^+$ has not been determined *in vivo*, but literature values for T_2 of other metabolites are in the 10 to 250 ms range [37,38]. This would lead to losses during preparation and readout for all forms of quantum filters. However, some of the short T_2 measurements are actually a reflection of the homonuclear couplings rather than the true T_2, so further investigation is needed [39]. Application to ADP may be more challenging, as a T_1 *in vivo* of only 870 ms has been measured at 9.4 T, but the relaxation times should be longer at lower field where there is less CSA relaxation.

In conclusion, we found that ^{31}P nuclear spin singlet states in ADP and NAD$^+$ have relatively short lifetimes, but such states can nevertheless be used to isolate the NMR spectral signature of these molecules. This result suggests there is utility in exploring singlet states even in systems where short lifetimes might be expected due to strong chemical shift anisotropy or out-of-pair couplings. In particular, when spin relaxation properties are sensitive to parameters such as pH, the T_s/T_1 ratio might also provide useful information about the chemical environment.

4. Methods

NMR spectroscopy was performed on a Bruker DMX 200 MHz spectrometer with a ^{1}H/X dual channel probe (81 MHz for ^{31}P). Reagents were purchased from Sigma Aldrich (St. Louis, MO, USA). ADP, ATP, and NAD$^+$ were in the form of sodium salts. For T_1 and T_S measurements, solutions were 50 mM of either ADP or NAD$^+$ in 69 mM pH 7.0 phosphate buffer (neutral conditions) or

Table 2
Phase list for the SUCCESS sequence (in degrees).

Step	1	2	3	4	5	6	7	8	9	10	11	12	13	14	15	16	17	18	19	20	21	22	23	24
ϕ_1	0	90	180	270	90	180	270	0	180	270	0	90	270	0	90	180	0	90	180	270	180	270	0	90
ϕ_3	0	0	0	0	90	90	90	90	180	180	180	180	270	270	270	270	0	0	0	0	180	180	180	180
ϕ_4	180	180	180	180	180	180	180	180	270	270	270	270	0	0	0	0	90	90	90	90	180	180	180	180
ϕ_{acq}	0	180	0	180	180	0	180	0	0	180	0	180	180	0	180	0	0	180	0	180	0	180	0	180

in 500 mM NaOH giving a pH > 13 (basic conditions). For SUCCESS measurements, a solution of 30 mM ATP, 3 mM ADP, and 3 mM NAD^+ was prepared in 69 mM pH 7.0 phosphate buffer. Conventional ^{31}P spectra were acquired with a 90-FID sequence, and T_1 was measured with a standard inversion recovery sequence. Chemical shifts were referenced to inorganic phosphate. T_S was measured with the SUCCESS sequence (below) using a series of spin-lock nutation times (τ_4). The ^{31}P spin-lock nutation frequency was 615 Hz. In all cases ^1H decoupling was applied during acquisition (CW, 150 Hz nutation frequency).

The SUCCESS technique has been described previously and is shown in Fig. 3 [21,26]. It is a Sarkar sequence combined with a filter for the singlet state (a type of zero-rank filter) [33]. In this pulse sequence, a singlet precursor state is prepared on a selected spin pair and CW decoupling is applied to create singlet order. A short sequence of hard pulses following a polyhedral phase cycle is then applied to create a quantum filter that passes only singlet order, which is then returned to transverse magnetization for readout. Pulse phases for ϕ_1, ϕ_3, ϕ_4, and ϕ_{acq} of the polyhedral phase cycle are given in Table 2. $\phi_2$was 0° throughout. The 24-phase cycle was chosen to ensure filtering of coherences up to rank $\lambda = 3$, the maximum possible for three spin-1/2 nuclei. Delay times for ADP were $\tau_1 = 12.02$ ms, $\tau_2 = 17.16$ ms, and $\tau_3 = 2.57$ ms. The center frequency was −10.74 ppm. For NAD^+, delays were $\tau_1 = 15.5$ ms, $\tau_2 = 16$ ms, and $\tau_3 = 12.5$ ms, and the center frequency was −11.675 ppm. For both molecules, the spin-locking time was $\tau_4 = 100$ ms and the spin-lock nutation frequency was $\nu_n = 615$ Hz. 8192 averages were taken with a delay of 14 s between measurements. A large number of averages were used for the SUCCESS demonstration so that residual ATP signal could be quantified. Metabolites were quantified in the reference and SUCCESS spectra by fitting each phased spectrum with Lorentzian lines. SUCCESS was also performed on the individual 50 mM ADP and NAD^+ solutions to quantify signal losses without interference from ATP.

Declaration of Competing Interest

The authors share royalty interest in U.S. Patent 20150042331 covering the SUCCESS method.

Acknowledgments

We acknowledge support from the NSF, Army, DARPA, and ARO MURI.

References

[1] D.L. Nelson, M.M. Cox, Lehninger Principles of Biochemistry, W. H. Freeman and Company, New York, 2005, pp. 496–507.
[2] M. Erecińska, I.A. Silver, ATP and Brain Function, J. Cereb. Blood Flow Metab. 9 (1989) 2–19, https://doi.org/10.1038/jcbfm.1989.2.
[3] E.N. Madonado, J.J. Lemasters, ATP/ADP Ratio, the Missed Connection between Mitochondria and the Warburg Effect, Mitochondrion 19 Pt A (2014) 78–84, https://doi.org/10.1016/j.mito.2014.09.002.
[4] M. Tantama, J.R. Martínez-François, R. Mongeon, G. Yellen, Imaging energy status in live cells with a fluorescent biosensor of the intracellular APT-to-ADP ratio, Nat. Commun. 4 (2013) 2550, https://doi.org/10.1038/ncomms3550.
[5] A.J. Covarrubias, R. Perrone, A. Grozio, E. Verdin, NAD^+ metabolism and its roles in cellular processes during ageing, Nat. Rev. Mol. Cell Biol. 22 (2021) 119–141, https://doi.org/10.1038/s41580-020-00313-x.
[6] B. Cuenoud, Ö. Ipek, M. Shevlyakova, M. Beaumont, S.C. Cunnane, R. Gruetter, L. Xin, Brain NAD is Associated with ATP Energy Production and Membrane Phospholipid Turnover in Humans, Front. Aging Neurosci. 12 (2020), https://doi.org/10.3389/fnagi.2020.609517 609517.
[7] M. Meyerspeer, C. Boesch, D. Cameron, M. Dezortová, S.C. Forbes, A. Heerschap, J.A.L. Jeneson, H.E. Kan, J. Kent, G. Layec, J.J. Prompers, H. Reyngoudt, A. Sleigh, L. Valkovič, G.J. Kemp, Experts' Working Group on ^{31}P MR Spectroscopy of Skeletal Muscle, 31P magnetic resonance spectroscopy in skeletal muscle: Experts' consensus recommendations, NMR Biomed. 34 (2021), https://doi.org/10.1002/nbm.4246 e4246.
[8] M.G. Stovell, J.-L. Yan, A. Sleigh, M.O. Mada, T.A. Carpenter, P.J.A. Hutchinson, K. L.H. Carpenter, Assessing Metabolism and Injury in Acute Human Traumatic Brain Injury with Magnetic Resonance Spectroscopy: Current and Future Applications, Front. Neurol. 8 (2017) 426, https://doi.org/10.3389/fneur.2017.00426.
[9] M.G. Stovell, M.O. Mada, T.A. Carpenter, J.-L. Yan, M.R. Guilfoyle, I. Jalloh, K.E. Welsh, A. Helmy, D.J. Howe, P. Grice, A. Mason, S. Giorgi-Coll, C.N. Gallagher, M. P. Murphy, D.K. Menon, P.J. Hutchinson, K.L.H. Carpenter, Phosphorus spectroscopy in acute TBI demonstrates metabolic changes that relate to outcome in the presence of normal structural MRI, J. Cereb. Blood Flow Metab. 40 (2020) 67–84, https://doi.org/10.1177/0271678X18799176.
[10] R. Skupienski, K.Q. Do, L. Xin, In vivo ^{31}P magnetic resonance spectroscopy study of mouse cerebral NAD content and redox state during neurodevelopment, Sci. Rep. 10 (2020) 15623, https://doi.org/10.1038/s41598-020-72492-8.
[11] A. Petersen, S.R. Kristensen, J.P. Jacobsen, M. Hørder, 31P-NMR measurements of ATP, ADP, 2,3-diphosphoglycerate and Mg2+ in human erythrocytes, Biochim. Biophys. Acta. 1035 (1990) 169–174, https://doi.org/10.1016/0304-4165(90)90112-a.
[12] Y. Lian, H. Jiang, J. Feng, X. Wang, X. Hou, P. Deng, Direct and simultaneous quantification of ATP, ADP and AMP by (1)H and (31)P Nuclear Magnetic Resonance spectroscopy, Talanta 150 (2016) 485–492, https://doi.org/10.1016/j.talanta.2015.12.051.
[13] A. Heerschap, C. Houtman, H. J. A. in 't Zandt, A. J. van den Bergh, B. Wieringa, Introduction to in vivo 31P magnetic resonance spectroscopy of (human) skeletal muscle, Proc. Nutr. Soc. 58 (1999) 861-870. https://doi.org/10.1017/S0029665199001160
[14] E. Hattingen, J. Magerkurth, U. Pilatus, A. Mozer, C. Seifried, H. Steinmetz, F. Zanella, R. Hilker, Phosphorus and proton magnetic resonance spectroscopy demonstrates mitochondrial dysfunction in early and advanced Parkinson's disease, Brain 132 (2009) 3285–3297, https://doi.org/10.1093/brain/awp293.
[15] R. Jayasundar, T.J. Norwood, L.D. Hall, N.M. Bleehen, Spectral editing techniques for 31P NMR spectroscopy of blood, Magn. Reson. Med. 10 (1989) 89–95, https://doi.org/10.1002/mrm.1910100108.
[16] Y.-L. Tsai, M.-W. Kao, S.-J. Huang, Y.-L. Lee, C.-P. Lin, J.C.C. Chan, Characterization of Phosphorus Species in Human Dentin by Solid-State NMR, Molecules 25 (2020) 196, https://doi.org/10.3390/molecules25010196.
[17] K.M. Brindle, M.B. Smith, B. Rajagopalan, G.K. Radda, Spectral Editing in ^{31}P NMR of Human Brain, J. Magn. Reson. 61 (1985) (1969) 559–563, https://doi.org/10.1016/0022-2364(85)90198-2.
[18] B.A. Berkowitz, Selective suppression of the ATP α- and γ-phosphate resonances in ^{31}P NMR, J. Magn. Reson. 91 (1991) (1969) 170–173, https://doi.org/10.1016/0022-2364(91)90421-O.
[19] D. Ben-Bashat, H. Shinar, G. Navon, 31P NMR Methods for the Direct Determination of ADP in the Presence of ATP, J. Magn. Reson. B 110 (1996) 231–239, https://doi.org/10.1006/jmrb.1996.0038.
[20] J. Ren, C.R. Malloy, A.D. Sherry, Quantitative measurement of redox state in human brain by 31P MRS at 7T with spectral simplification and inclusion of multiple nucleotide sugar components in data analysis, Magn. Reson. Med. 84 (2020) 2338–2351, https://doi.org/10.1002/mrm.28306.
[21] S.J. DeVience, R.L. Walsworth, M.S. Rosen, Nuclear spin singlet states as a contrast mechanism for NMR spectroscopy, NMR Biomed. 26 (2013) 1204–1212, https://doi.org/10.1002/nbm.2936.
[22] A.S. Kiryutin, H. Zimmerman, A.V. Yurkovskaya, H.-M. Vieth, K.L. Ivanov, Long-lived spin states as a source of contrast in magnetic resonance spectroscopy and imaging, J. Magn. Reson. 261 (2015) 64–72, https://doi.org/10.1016/j.jmr.2015.10.004.
[23] S. Mamone, N. Rezaei-Ghaleh, F. Opazo, C. Griesinger, S. Glöggler, Singlet-filtered NMR spectroscopy, Sci. Adv. 6 (2020) eaaz1955, https://doi.org/10.1126/sciadv.aaz1955.

[24] S. Mamone, A.B. Schmidt, N. Schwaderlapp, T. Lange, D. von Elverfeldt, J. Hennig, S. Glöggler, Localized singlet-filtered MRS in vivo, NMR Biomed. 34 (2021), https://doi.org/10.1002/nbm.4400 e4400.
[25] A.N. Pravdivtsev, F.D. Sönnichsen, J.-B. Hövener, In vitro singlet state and zero-quantum encoded magnetic resonance spectroscopy: Illustration with N-acetylaspartate, PLoS ONE 15 (2020), https://doi.org/10.1371/journal.pone.0239982 e0239982.
[26] G. Pileio, M.H. Levitt, Isotropic filtering using polyhedral phase cycles: application to singlet state NMR, J. Magn. Reson. 191 (2008) 148–155, https://doi.org/10.1016/j.jmr.2007.11.021.
[27] G. Pileio, Relaxation theory of nuclear singlet states in two spin-1/2 systems, Prog. Nucl. Magn. Reson. Spectrosc. 56 (2010) 217–231, https://doi.org/10.1016/j.pnmrs.2009.10.001.
[28] H. Majd, M. S. King, S. M. Palmer, A. C. Smith, L. D. H. Elbourne, I. T. Paulsen, D. Sharples, P. J. F. Henderson, E. R. S. Kunji, Screening of candidate substrates and coupling ions of transporters by thermostability shift assays, eLife, 7 (2018) e38821. https://doi.org/10.7554/eLife.38821.001
[29] K.G. Devine, S. Jheeta, De Novo Nucleic Acids: A Review of Synthetic Alternatives to DNA and RNA That Could Act as Bio-Information Storage Molecules, Life 10 (2020) 346, https://doi.org/10.3390/life10120346.
[30] R.A. Alberty, R.N. Goldberg, Standard thermodynamic formation properties for the adenosine 5'-triphosphate series, Biochem. 31 (1992) 10610–10615, https://doi.org/10.1021/bi00158a025.
[31] D. E. Korenchan, J. Lu, M. H. Levitt, A. Jerschow, ^{31}P nuclear spin singlet lifetimes in a system with switchable magnetic inequivalence: experiment and simulation, Phys. Chem. Chem. Phys. (2021) Advance Article. https://doi.org/10.1039/D1CP03085J
[32] Y. Feng, T. Theis, X. Liang, Q. Wang, P. Zhou, W.S. Warren, Storage of Hydrogen Spin Polarization in Long-Lived $^{13}C_2$ Singlet Order and Implications for Hyperpolarized Magnetic Resonance Imaging, J. Am. Chem. Soc. 135 (2013) 9632–9635, https://doi.org/10.1021/ja404936p.
[33] R. Sarkar, P.R. Vasos, G. Bodenhausen, Singlet-state exchange NMR spectroscopy for the study of very slow dynamic processes, J. Am. Chem. Soc. 129 (2007) 328–334, https://doi.org/10.1021/ja0647396.
[34] M.C.D. Tayler, M.H. Levitt, Singlet nuclear magnetic resonance of nearly-equivalent spins, Phys. Chem. Chem. Phys. 13 (2011) 5556–5560, https://doi.org/10.1039/C0CP02293D.
[35] S.J. DeVience, R.L. Walsworth, M.S. Rosen, Preparation of Nuclear Spin Singlet States Using Spin-Lock Induced Crossing, Phys. Rev. Lett. 111 (2013), https://doi.org/10.1103/PhysRevLett.111.173002 173002.
[36] A.N. Pravdivtsev, A.S. Kiryutin, A.V. Yurkovskaya, H.-M. Vieth, K.L. Ivanov, Robust conversion of singlet spin order in coupled spin-1/2 pairs by adiabatically ramped RF-fields, J. Magn. Reson. 273 (2016) 56–64, https://doi.org/10.1016/j.jmr.2016.10.003.
[37] W. M. Brooks, J. Field, M. G. Irving, D. M. Doddrell, In vivo determination of 31P spin relaxation times (T1, T2, T1rho) in rat leg muscle. Use of an off-axis solenoid coil, Magn. Reson. Imaging 4 (1986) 245-250. https://doi.org/10.1016/0730-725x(86)91065-9
[38] W.J.M. van der Kemp, D.W.J. Klomp, J.P. Wijnen, ^{31}P T_2s of Phosphomonoesters, Phosphodiesters, and Inorganic Phosphate in the Human Brain at 7T, Magn. Reson. Med. 80 (2018) 29–35, https://doi.org/10.1002/mrm.27026.
[39] W.-I. Jung, K. Straubinger, M. Bunse, S. Widmaier, F. Schick, K. Küper, G. Dietze, O. Lutz, A Pitfall Associated with Determination of Transverse Relaxation Times of the ^{31}P NMR Signals of ATP Using the Hahn Spin-Echo, Magn. Reson. Med. 30 (1993) 138–141, https://doi.org/10.1002/mrm.1910300122.